

## The ballasting effect of Saharan dust deposition on aggregate dynamics and carbon export: Aggregation, settling, and scavenging potential of marine snow

Helga van der Jagt <sup>1,2</sup> Carmen Friese,<sup>2</sup> Jan-Berend W. Stuur <sup>2,3</sup> Gerhard Fischer,<sup>2,4</sup>  
Morten H. Iversen <sup>1,2\*</sup>

<sup>1</sup>Helmholtz Young Investigator Group SEAPUMP, Alfred Wegener Institute for Polar and Marine Research, Bremerhaven, Germany

<sup>2</sup>MARUM, Center for Marine Environmental Sciences, University of Bremen, Bremen, Germany

<sup>3</sup>NIOZ-Royal Netherlands Institute for Sea Research, and Utrecht University, Den Burg, The Netherlands

<sup>4</sup>Geosciences Department, University of Bremen, Bremen, Germany

### Abstract

Lithogenic material such as Saharan dust can be incorporated into organic aggregates and act as ballast, potentially enhancing the marine carbon export via increased sinking velocities of aggregates. We studied the ballasting effects of Saharan dust on the aggregate dynamics in the upwelling region off Cape Blanc (Mauritania). Aggregate formation from a natural plankton community exposed to Saharan dust deposition resulted in higher abundance of aggregates with higher sinking velocities compared to aggregate formation with low dust. This higher aggregate abundance and sinking velocities potentially increased the carbon export 10-fold when the aggregates were ballasted by Saharan dust. After aggregate formation in the surface waters, subsequent sinking through suspended Saharan dust minerals had no influence on aggregate sizes, abundance, and sinking velocities. We found that aggregates formed in the surface ocean off Mauritania were already heavily ballasted with lithogenic material and could therefore not scavenge any additional minerals during their descent. This suggests that carbon export to the deep ocean in regions with high dust deposition is strongly controlled by dust input to the surface ocean while suspended dust particles in deeper water layers do not significantly interact with sinking aggregates.

Carbon export is driven by the formation and sinking of aggregated organic material into the deep ocean. The time period for which carbon is stored in the ocean depends on the depth of remineralization, and only organic matter reaching the bathypelagic will be stored in the ocean for centuries (Lampitt et al. 2008). Fast sinking aggregates remain shorter in the upper ocean, are degraded less and therefore more likely to reach the deep ocean (Iversen and Ploug 2013). Therefore an increased sinking velocity will increase the depth of remineralization and, thus, the carbon export efficiency (Allredge and Silver 1988; Allredge and Jackson 1995).

The downward fluxes of biogenic and lithogenic minerals, such as silicate, carbonate and Saharan dust, are often closely

correlated to particulate organic carbon (POC) fluxes (Armstrong et al. 2002; Francois et al. 2002; Klaas and Archer 2002). It has been hypothesized that these minerals are incorporated as ballast into aggregates, resulting in increased sinking velocities. This incorporation can take place during the formation of aggregates in the surface and subsurface ocean or when aggregates “scavenge” dust particles while sinking (Passow and De La Rocha 2006). Incorporation of ballast minerals into aggregates has been observed to enhance aggregate formation, increase size-specific sinking velocities but also to fragment large aggregates into smaller ones (Hamm 2002; Passow and De La Rocha 2006; Engel et al. 2009<sup>a,b</sup>; Lee et al. 2009; Iversen and Robert 2015). Ballasted aggregates are remineralized at the same rate as non-ballasted aggregates (Ploug et al. 2008<sup>b</sup>; Iversen and Ploug 2010), but due to their increased size-specific sinking velocities they are likely to be remineralized at greater depth than non-ballasted aggregates. However, most direct studies of the influence of ballast minerals on organic aggregates have been done in the laboratory with phytoplankton cultures (e.g., Hamm 2002; Passow and De La Rocha 2006; Iversen and Ploug 2010).

Ballast minerals can be incorporated into aggregates during aggregate formation in the surface ocean, or when aggregates

\*Correspondence: morten.iversen@awi.de

<https://doi.pangaea.de/10.1594/PANGAEA.885930>

This is an open access article under the terms of the Creative Commons Attribution-NonCommercial-NoDerivs License, which permits use and distribution in any medium, provided the original work is properly cited, the use is non-commercial and no modifications or adaptations are made.

“scavenge” suspended minerals during their descent into the bathypelagic. Scavenging depends on the concentration, size, and sinking velocity of both aggregates and ballast minerals as well as on the stickiness of the aggregates (Simon et al. 2002; Burd and Jackson 2009). Transparent exopolymer particles (TEP) determine the stickiness of aggregates (Alldredge et al. 1993; Engel 2000), but TEP may become saturated with ballast minerals and therefore lose its stickiness (Passow 2004). Porous aggregates may have fluid flow through them, which could contribute to efficient scavenging of small suspended or slow-sinking particles (Stolzenbach 1993; Li and Logan 1997, 2000) which has been observed for porous aggregates collected in the Baltic (Ploug et al. 2002). However, it is unclear if compact, ballasted aggregates from regions with high concentrations of ballast minerals scavenge lithogenic particles at depth (Iversen et al. 2010), since large sinking particles push water away and limits the scavenging potential (Kiorboe 2008).

Several studies have observed that detached suspended particles from the shelf and upper slope regions extent horizontally offshore as large slow-sinking plumes of fine particles, that are often referred to as intermediate nepheloid layers (INLs) (Dickson and McCave 1986; Hall et al. 2000; Frignani et al. 2002). INLs are a general feature in upwelling regions where intensification of bottom currents and internal waves generate INLs through changes in water density gradients caused by the upwelling (Dickson and McCave 1986). INLs are a prominent feature in the high productive Eastern Boundary Upwelling area off Cape Blanc, Mauritania, where erosion from the shelf sediment generates particle plumes in subsurface layers (Karakas et al. 2006; Fischer et al. 2009; Iversen et al. 2010). The INLs are typically observed with optical systems between 200 m and 600 m depth near-shore (Nowald et al. 2006; Iversen et al. 2010) while they slowly deepen with sinking velocities of  $\sim 5 \text{ m d}^{-1}$  as they are advected off-shore via Ekman transport (Karakas et al. 2006). Very little is known about the particle composition of the INLs, except that they are formed from slowly sinking material, which could originate from eroded shelf sediment and/or dust deposition of slow sinking particles near the coast. It has been suggested that there is little interaction between vertically settling marine snow and INLs in the region off Cape Blanc (Karakas et al. 2006; Iversen et al. 2010). On the other hand, several studies have suggested that the vertical flux of organic matter is strongly influenced by Saharan dust deposition to the surface water (Fischer and Karakas 2009; Iversen et al. 2010; Nowald et al. 2015). Especially peak flux events off Cape Blanc seem to follow distinct dust outbreaks during winter and summer (Nowald et al. 2015; Fischer et al. 2016), but it still remains unclear whether these dust outbreaks cause higher aggregate formation in the surface waters or if the deposited dust is scavenged by already formed aggregates.

During a cruise off Cape Blanc, Mauritania we performed on-board incubations, using in situ collected marine snow, a

natural phytoplankton community and Saharan dust. We found that Saharan dust enhanced the formation of aggregates and increased their sinking velocities. However, we did not find any indications of particle scavenging by already formed aggregates.

## Material and methods

We studied the influence of Saharan dust on the formation and settling of aggregates during the RV *Poseidon* cruise (POS481) from 15 February 2015 to 03 March 2015 off Cape Blanc, Mauritania. We performed two experiments to investigate the effect of dust deposition on the formation of aggregates, using a natural plankton community exposed to both high and low concentrations of added Saharan dust. Additionally, we performed one experiment to investigate the scavenging potential of sinking aggregates, by incubating in situ collected aggregates with and without added dust.

### Aggregate formation experiments

For the two formation experiments, seawater was collected from the fluorescence maximum depth at 20 m with a CTD-rossette sampler. The collected water was incubated with and without added dust, and repeated for a high and low dust deposition ( $4.2 \text{ mg L}^{-1}$  and  $1.4 \text{ mg L}^{-1}$ , respectively). The experiment on the effect of high dust deposition was done at  $21^{\circ}18.9'N$   $20^{\circ}50.34'W$  and the experiment on the effect of low dust deposition was done at  $20^{\circ}51.87'N$   $18^{\circ}57.08'W$  (Fig. 1). Both studies were carried out by filling 10 roller tanks (1.15 L, diameter: 14 cm, depth: 7.5 cm) with fluorescence maximum water, and adding a dust suspension to five of the tanks. The tanks without dust additions received a blank solution of GF/F filtered seawater of the same volume as the dust additions. The roller tanks were placed on a roller table rotating with a speed of 3 RPM for

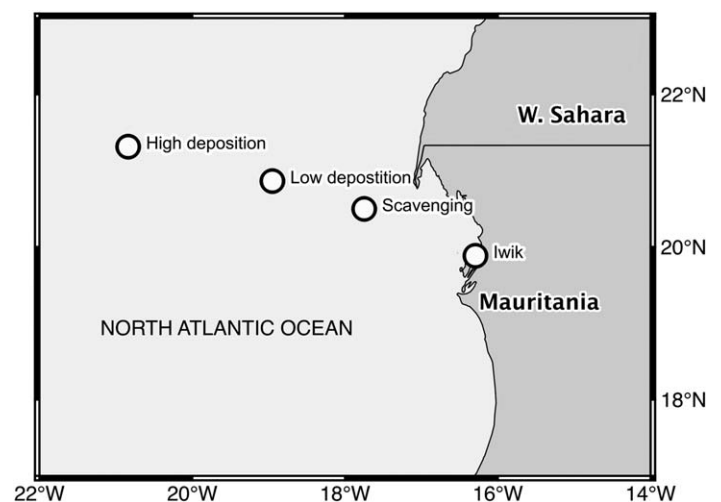


**Fig. 1.** Overview of the locations of the high dust deposition, low dust deposition, and scavenging experiment, and dust collection location Iwik.

**Table 1.** Equivalent spherical diameter (ESD), number of formed aggregates per liter, total aggregated volume and sinking velocity for the high deposition, low deposition and scavenging experiments. Average  $\pm$  SD.

| Experiment      |         | ESD<br>(mm)     | Total agg.<br>(# L <sup>-1</sup> ) | Total agg. vol.<br>(mm <sup>3</sup> L <sup>-1</sup> ) | Sinking velocity<br>(m d <sup>-1</sup> ) |
|-----------------|---------|-----------------|------------------------------------|---|--|
| High deposition | Control | 0.52 $\pm$ 0.30 | 5.04 $\pm$ 3.71                    | 0.79 $\pm$ 0.48                                       | 133 $\pm$ 108                            |
|                 | Dust    | 0.62 $\pm$ 0.51 | 16.87 $\pm$ 9.21                   | 8.98 $\pm$ 3.11                                       | 430 $\pm$ 280                            |
| Low deposition  | Control | 1.45 $\pm$ 0.78 | 4.35 $\pm$ 2.84                    | 3.43 $\pm$ 4.47                                       | 42 $\pm$ 23                              |
|                 | Dust    | 0.75 $\pm$ 0.61 | 23.04 $\pm$ 6.60                   | 71.88 $\pm$ 22.81                                     | 109 $\pm$ 42                             |
| Scavenging      | Control | 1.29 $\pm$ 0.85 | 6.09 $\pm$ 3.14                    | 17.10 $\pm$ 5.64                                      | 319 $\pm$ 210                            |
|                 | Dust    | 1.40 $\pm$ 0.80 | 5.51 $\pm$ 3.05                    | 17.21 $\pm$ 6.81                                      | 403 $\pm$ 280                            |

36 h in darkness at in situ temperature (19°C) to allow aggregate formation. We collected all the formed aggregates individually and measured their size and sinking velocity in a vertical flow chamber (*see* Ploug and Jørgensen 1999). Each measured aggregate was frozen individually at  $-20^{\circ}\text{C}$  for further analysis in the home laboratory.

#### Scavenging experiment

To study how settling aggregates scavenge dust when they sink through the water column, we collected in situ marine snow aggregates with a Marine Snow Catcher (MSC). The MSC can sample intact in situ formed aggregates, which allows studying the composition, size and sinking velocity of natural aggregates from different water depths (Riley et al. 2012). The aggregates were collected below the fluorescence maximum layer at a depth of 60 m at  $20^{\circ}29.97'\text{N}$   $17^{\circ}44.98'\text{W}$ . We divided all collected aggregates evenly into eight roller tanks that were filled with GF/F filtered seawater from the MSC, and added the low dust suspension to four of the roller tanks, while the other four received a 1 mL blank solution. The roller tanks were placed on a roller table rotating with 3 RPM for 24 h in darkness to allow dust scavenging by the incubated aggregates. Afterwards, all aggregates were collected individually, and their size and sinking velocities were determined in the flow chamber (Ploug and Jørgensen 1999). Each measured aggregate was frozen individually at  $-20^{\circ}\text{C}$  for further analysis in the home laboratory.

#### Dust suspensions

To generate the dust suspensions, we collected Saharan dust with modified Wilson and Cooke samplers (Wilson and Cooke 1980; Mendez et al. 2011), which collected wind-transported dust in the Banc d'Arguin National Park in Mauritania ( $\sim 19^{\circ}53'\text{N}$ ,  $\sim 16^{\circ}18'\text{W}$ ) during 2013 (Friese et al. 2017). These passive samplers are used to collect material transported by wind (dry deposition), and consist of a plastic bottle with an in- and outlet tube that are placed in the wind. Dust particles entering the sampler via the inlet tube settle into the bottle due to a pressure drop caused by a difference in diameter between the inlet tube and bottle, and clean air leaves the bottle via the outlet. The sampling efficiency of a modified Wilson and Cooke sampler is 90%

(Goossens and Offer 2000). The sampling bottles were attached to a mast at 290 cm above the ground and were replaced every month; the collected dust was stored dry and dark. Dust collected in August was used for the high dust deposition experiment, and dust collected in April was used for the low dust deposition and scavenging experiment. We determined the grain-size distribution of the two dust suspensions using a Beckmann Coulter laser particle sizer (LS 13 320) equipped with a Micro Liquid Module (MLM, analytical error of  $\pm 1.26\ \mu\text{m}$  ( $\pm 4.00\%$ ), *see* Friese et al. 2016, 2017). The peak in the particle diameter frequency (given in volume %) was at  $30\ \mu\text{m}$  for both samples, which was similar to Saharan dust collected with deep sea sediment traps off Cape Blanc (Friese et al. 2016). Microscopic observations using a Zeiss Axioskop 40 polarizing microscope revealed that the two dust suspensions were of similar composition with the dominant minerals being quartz, carbonate, and clay minerals with minor contributions of hematite and calcite.

The collected dust samples were suspended in 10 mL distilled water and mixed thoroughly before allowing a 5 s resting period to let the fast-sinking particles settle out, and then removing 5 mL of the suspended dust. The resting period was to prevent that the dust suspension would contain very fast-sinking dust particles, which would have settled out individually after deposition. We mixed the dust suspension with GF/F-filtered seawater before adding the solution to the roller tanks. The experiments with high dust deposition contained  $4.2\ \text{mg dust L}^{-1}$ , and the low dust deposition contained  $1.4\ \text{mg dust L}^{-1}$ .

#### Dry weight and POC

We filtered 2 L water used for the aggregation experiments onto combusted pre-weighed GF/F filters to determine dry weight and particulate organic carbon (POC). To determine the POC per aggregate for each treatment, one to four aggregates of similar sizes were filtered onto pre-combusted GF/F filters. The filters were gently washed with demineralized water, dried at  $40^{\circ}\text{C}$  for 24 h and re-weighed to obtain the dry weight before removing inorganic carbon ( $\text{CaCO}_3$ ) by fuming with 37% HCl and analyzed with a GC elemental analyzer (Elementar vario EL III) to obtain the POC values. We pooled aggregates into size classes where possible.

**Excess density**

The excess density was calculated using the Navier-Stokes drag equation, as described in Iversen and Ploug (2010):

$$\Delta\rho = \frac{C_D \rho_w w^2}{\frac{4}{3} g \text{ESD}} \quad (1)$$

Where  $C_D$  is the dimensionless drag force:

$$C_D = \frac{24}{Re} + \frac{6}{1 + Re^{0.5}} + 0.4 \quad (2)$$

And Reynolds number ( $Re$ ):

$$Re = w \text{ESD} \frac{\rho_w}{\eta} \quad (3)$$

$\rho_w$  is the density of seawater at 19°C with a salinity of 36 psu (1.0258 g cm<sup>-3</sup>),  $\eta$  the dynamic viscosity (1.0610·10<sup>-2</sup> g cm<sup>-1</sup> s<sup>-1</sup>)  $w$  the sinking velocity in cm s<sup>-1</sup>,  $g$  the gravitational acceleration (981 cm s<sup>-2</sup>), and ESD the equivalent spherical diameter in cm.

**Statistical analysis**

Statistics was performed in R (R Core Team 2016). Differences in the relation between ESD vs. sinking velocity and excess density between control and treatment were calculated using a linear model that estimated both intercept and slope for each group. The data were log-log transformed prior to analysis to assume linearity. Afterwards, 95% confidence intervals were calculated for each predicted parameter. If the CI's for one of the parameters did not overlap, the groups were determined as significantly different. All other data were first tested for normality using a Shapiro–Wilk Normality Test, after which either a two-sample  $t$ -test or a non-parametric Wilcoxon signed-rank test were used.

**Results**

**Aggregate formation and settling after dust deposition**

The POC concentrations of the water collected from the fluorescence maximum were 0.17 mg L<sup>-1</sup> for the high dust deposition experiment and 0.15 mg L<sup>-1</sup> for the low dust deposition. The total dry weight was 3.14 mg L<sup>-1</sup> and 1.29 mg L<sup>-1</sup>, respectively, suggesting that the water used for the high dust deposition contained more inorganic material than that used for the low dust deposition experiment. The aggregates formed during high dust deposition were smaller and sank faster than those formed during low dust deposition (Table 1, Wilcoxon rank sum test,  $p < 0.01$ ). Excess density decreased with increasing size for all treatments, due to the fractal nature and porosity of the aggregates (Fig. 3d–f).

In the high dust deposition experiment, aggregates already formed after 12 h when dust was added, while it took 24 h before the first visible aggregates were observed in the treatments without dust additions. The total aggregated volume and the number of aggregates formed were

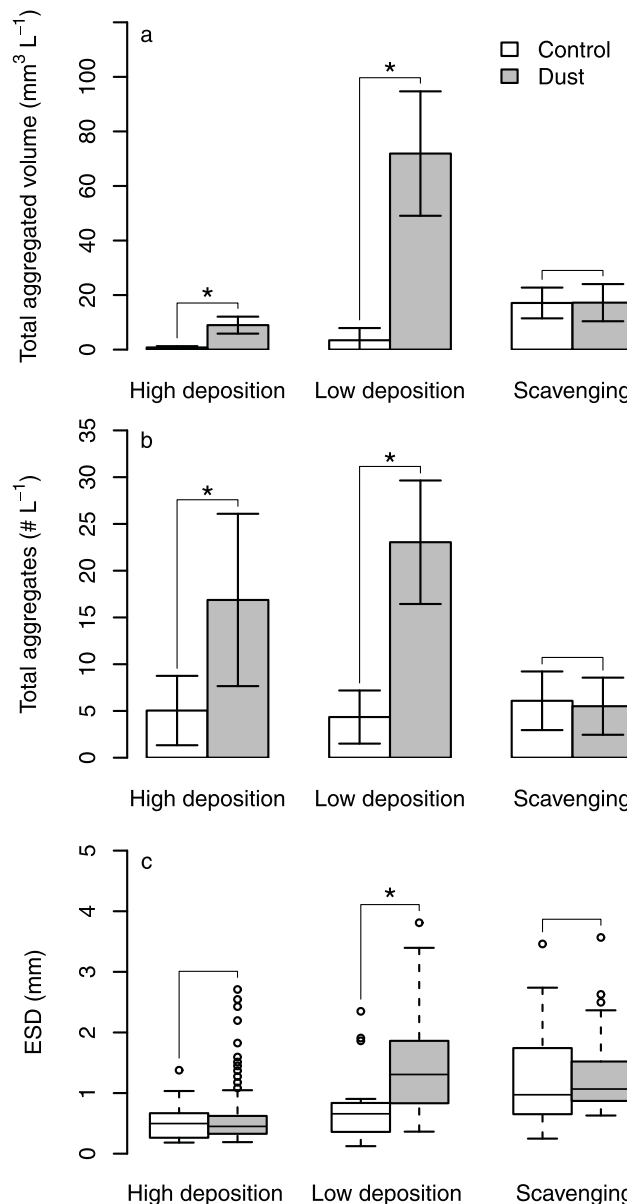


**Fig. 2.** (a) Total aggregated volume per liter for the three experiments, asterisks indicate significant differences (two-sample  $t$ -test,  $p < 0.01$ ,  $p < 0.01$ , and  $p = 0.98$ , respectively). Average  $\pm$  SD; (b) number of aggregates formed per liter, asterisks indicate significant differences (two-sample  $t$ -test,  $p = 0.04$ ,  $p < 0.01$ , and  $p = 0.83$ , respectively). Average  $\pm$  SD; and (c) box-whisker plots of aggregate sizes, asterisks indicates significance (Wilcoxon rank sum test,  $p = 0.72$ ,  $p < 0.01$ , and  $p = 0.53$ , respectively).

significantly higher in the dust treatment compared to the control treatment without dust (Fig. 2a,b, two-sampled  $t$ -test,  $p < 0.01$  and  $p = 0.04$ , respectively). The ESD of the aggregates formed in the treatment exposed to high dust deposition was not significantly different from the average ESD of the aggregates formed in the control treatment (Fig. 2c, Wilcoxon rank sum test,  $p = 0.72$ ). The aggregates formed

**Table 2.** Dry weight and POC values per size class per experiment. Number of measured aggregates (Agg #), average ESD  $\pm$  SD, POC per volume ratio (POC : V), dry weight per volume ratio (DW : V) and POC per dry weight ratio (POC : DW).

| Experiment      |         | Agg # | ESD $\pm$ SD (mm) | POC : V ( $\mu\text{g C mm}^{-3}$ ) | DW : V ( $\mu\text{g mm}^{-3}$ ) | POC : DW % |
|-----------------|---------|-------|-------------------|-------------------------------------|----------------------------------|------------|
| High deposition | Control | 14    | 0.33 $\pm$ 0.13   | n.a.                                | 3696                             | n.a.       |
|                 |         | 4     | 0.98 $\pm$ 0.32   | 9.83                                | 192                              | 5.13       |
|                 | Dust    | 10    | 0.39 $\pm$ 0.09   | 61.42                               | 4495                             | 1.37       |
|                 |         | 10    | 0.57 $\pm$ 0.27   | 19.21                               | 1361                             | 1.41       |
|                 |         | 2     | 1.71 $\pm$ 0.16   | 4.84                                | 221                              | 2.19       |
| Low deposition  | Control | 9     | 0.44 $\pm$ 0.27   | 26.79                               | 1347                             | 1.99       |
|                 |         | 1     | 1.86              | 1.48                                | 58                               | 2.57       |
|                 | Dust    | 10    | 0.91 $\pm$ 0.30   | 5.38                                | 367                              | 1.47       |
|                 |         | 1     | 1.64              | 5.10                                | n.a.                             | n.a.       |
|                 |         | 2     | 2.13 $\pm$ 1.32   | 0.61                                | 64                               | 0.95       |
| Scavenging      | Control | 6     | 0.57 $\pm$ 0.24   | 25.09                               | 3705                             | 0.68       |
|                 |         | 5     | 0.96 $\pm$ 0.19   | 4.99                                | 239                              | 2.09       |
|                 |         | 6     | 2.06 $\pm$ 0.78   | 1.28                                | 45                               | 2.83       |
|                 | Dust    | 5     | 0.76 $\pm$ 0.12   | 8.63                                | 941                              | 0.92       |
|                 |         | 3     | 1.02 $\pm$ 0.06   | 5.06                                | 381                              | 1.33       |
|                 |         | 4     | 1.45 $\pm$ 0.13   | 2.28                                | 143                              | 1.59       |
|                 |         | 3     | 2.50 $\pm$ 0.13   | 0.82                                | 41                               | 2.00       |

n.a., not available.

in the dust treatment had a lower POC to dry weight ratio and a higher dry weight to volume ratio (Table 2), indicating that they contained a higher amount of inorganic mineral particles compared to control aggregates. The size-specific sinking velocities of the aggregates formed with added dust were significantly faster than those formed without dust additions (Fig. 3a, linear regression on log-transformed data,  $p < 0.01$ ). Also the excess density to size relation was different, the excess density of aggregates formed with added dust were significantly higher (Fig. 3d, linear regression on log-transformed data,  $p < 0.01$ ).

The low dust deposition experiment showed higher total aggregated volume and numbers of aggregates formed with dust added compared to the aggregates formed without dust additions (Fig. 2a,b, two-sample  $t$ -test,  $p < 0.01$ ). The aggregates formed in the dust-treatment had higher size-specific sinking velocities than those formed without added dust (Fig. 3b, linear regression on log-transformed data,  $p < 0.01$ ), and excess densities were significantly higher (Fig. 3e, linear regression on log-transformed data,  $p < 0.01$ ). Contrary to the high dust deposition experiment, the aggregates formed with added dust were significantly larger than those formed without added dust (Fig. 2c, Wilcoxon rank sum test,  $p < 0.01$ ). The POC to volume ratio and the POC to dry weight ratio was generally higher for control aggregates (Table 2).

To study the natural occurrence of minerals within the aggregates formed from the incubations without dust additions, we performed microscopic observation using a Zeiss

Axioskop 40 polarizing microscope. This showed that the aggregates formed from the in situ collected water without dust contained quartz and clay minerals, suggesting that dust was already present in the natural sea water samples.

#### Size, volume, and sinking velocity of scavenging aggregates

We did not observe any difference between in situ collected aggregates after incubating them in roller tanks with and without added dust. The total aggregated volume and total amount of aggregates per liter was the same for the treatments with and without dust after 24 h incubation in roller tanks (Fig. 2a,b; Table 1, two-sampled  $t$ -test,  $p = 0.98$  and  $p = 0.83$ , respectively). We also did not observe any differences between average ESD of the aggregates (Fig. 2c, Wilcoxon signed rank test,  $p = 0.46$ ), between the relationship between size and sinking velocity (Fig. 3, linear regression on log-transformed data,  $p = 0.53$ ) or between the average POC to dry weight ratios between the dust and control treatment after the 24 h of incubation (Table 2).

#### Discussion

We observed that addition of Saharan dust enhanced aggregate formation from a natural plankton community and resulted in higher aggregate abundance. The formed aggregates had higher size-specific sinking velocities compared to those formed in situations without dust addition. This supports previous observations from laboratory experiments where inclusion of minerals into organic aggregates

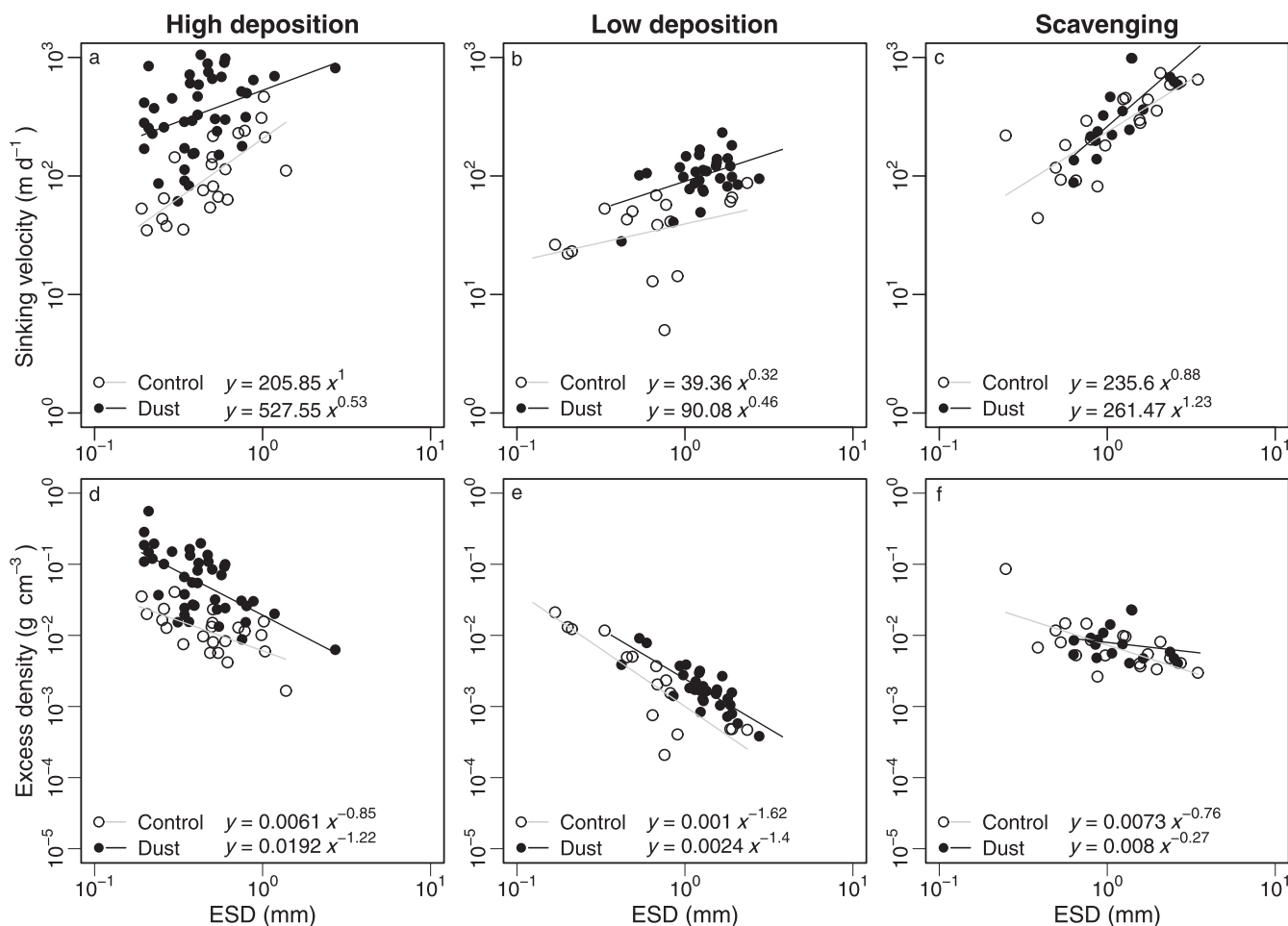


**Fig. 3.** Size vs. sinking velocity and excess density of all measured aggregates, in combination with the fitted regression lines. (a, d) Aggregates formed under high dust deposition (linear regression on logtransformed data,  $p < 0.01$ ); (b, e) aggregates formed under low dust deposition ( $p < 0.01$ ); and (c, f) in situ aggregates sinking through suspended dust ( $p = 0.53$ ).

increased aggregate formation, abundance, and size-specific sinking velocities compared to incubations without minerals (Hamm 2002; Passow and De La Rocha 2006; Iversen and Robert 2015). So far, no studies have observed an influence from ballast minerals on microbial degradation (Ploug et al. 2008a,b; Iversen and Ploug 2010; Iversen and Robert 2015), suggesting that the increased aggregate formation and higher sinking velocities may lead to an increased POC flux in dusty regions. This effect was directly shown in mesocosm experiments in the Mediterranean Sea, where an input of Saharan dust resulted in two to six times higher POC flux (Bressac et al. 2014), and indirectly with sediment traps recording increased POC fluxes with dust deposition (Ternon et al. 2010; Fischer et al. 2016; Pabortsava et al. 2017). Our results show that dust deposition caused a 10-fold increase in total aggregated volume and two-fold higher size-specific sinking velocities of the dust-ballasted aggregates. On the other hand, the dust-ballasted aggregates had half the amount of volumetric POC compared to non-ballasted aggregates. Still,

due to the high aggregate abundance and sinking velocities of the ballasted aggregates, a dust deposition may cause up to 10-fold higher POC flux.

In ballasting experiments conducted with phytoplankton from cultures, mineral ballasting increased aggregate fragmentation and aggregate compactness, resulting in smaller aggregates (Hamm 2002; Passow and De La Rocha 2006; Ploug et al. 2008a). However, in our experiments we did not observe changes in size of the aggregates formed with and without additional dust. Still, there is Saharan dust deposition to the surface waters off Cape Blanc almost year-round (Iversen et al. 2010; Fischer et al. 2016; Friese et al. 2016), and it is therefore likely that the aggregates formed with water from the fluorescence maximum were already ballasted. Nowald et al. (2015) made video observations of settling aggregates in the deep ocean off Cape Blanc and found that in situ aggregate sizes remained small throughout the year (mostly with a diameter of  $\sim 1$  mm) and that Saharan dust deposition only increased aggregate abundance without

having any effect on aggregate size. It therefore seems that peak fluxes due to dust deposition off Cape Blanc is driven by the formation of many small and dense aggregates rather than by a few large aggregates (Nowald et al. 2015).

When we exposed in situ collected aggregates to suspended Saharan dust, we did not observe any changes in aggregate sizes, abundance, or size-specific sinking velocities, indicating that these aggregates did not scavenge suspended dust. The scavenging potential of an aggregate may be determined by its stickiness, which is in turn controlled by the amount of transparent exopolymer particles (TEP) (Allredge et al. 1993; Engel 2000). However, TEP may become saturated with particles and lose its stickiness, resulting in a reduced scavenging potential (Passow 2004). It has been suggested that the carrying capacity for minerals by aggregates is limited to 95% of the aggregate's dry weight made up by inorganic components (Passow 2004). We found that organic carbon only contributed with maximum 5% to the total dry weight of the in situ formed aggregates, suggesting that the carrying capacity for Saharan dust was already saturated when we exposed them to additional Saharan dust. This would explain why we did not observe scavenging of the added dust by the in situ collected aggregates. Further, this also implies that aggregates formed in surface waters with high dust depositions become ballasted during their formation and may reach their maximum carrying capacity before they sink to the deeper water column. This prevents scavenging of lithogenic material in the deep ocean and could explain the persistence of large nepheloid layers in productive regions such as the upwelling area off Cape Blanc (Fischer et al. 2009). These nepheloid layers are still observed after large export events during winter and spring (Karakas et al. 2006), and do not significantly alter aggregate size-distribution and abundance of aggregates that sink through these layers (Iversen et al. 2010). This suggests little interaction between export production and the nepheloid layers.

Two possible, but contrasting, scenarios have been suggested for the future oceans; (1) increasing dust deposition due to future desertification and stronger trade winds (e.g., Naiman 1976; Shao et al. 2011) and (2) Saharan "greening" will limit dust emissions from source regions and cause less dust deposition in the future oceans (Fontaine et al. 2011; Lucio et al. 2012). A change in dust deposition may have profound effects on the global ocean due to the fertilizing effect of dust-originating nutrients on primary producers (Jickells et al. 2005; Ridame et al. 2014), especially of iron in high latitude regions. However, the role of dust as ballast material and therefore its effects on the downward carbon flux is often overlooked in global ocean models (e.g., McTainsh and Strong 2007; Maher et al. 2010). We show that the ballasting effect of dust deposition to the surface ocean also has a profound effect on POC export in productive lower latitude regions, while there was no evidence for scavenging of mineral dust by already ballasted aggregates.

## References

- Allredge, A. L., and M. W. Silver. 1988. Characteristics, dynamics and significance of marine snow. *Prog. Oceanogr.* **20**: 41–82. doi:10.1016/0079-6611(88)90053-5
- Allredge, A. L., U. Passow, and B. E. Logan. 1993. The abundance and significance of a class of large, transparent organic particles in the ocean. *Deep-Sea Res. I* **40**: 1131–1140. doi:10.1016/0967-0637(93)90129-Q
- Allredge, A. L., and G. A. Jackson. 1995. Aggregation in marine systems. *Deep-Sea Res. II* **42**: 1–7. doi:10.1016/0967-0645(95)90003-9
- Armstrong, R. A., C. Lee, J. I. Hedges, S. Honjo, and S. G. Wakeham. 2002. A new, mechanistic model for organic carbon fluxes in the ocean based on the quantitative association of POC with ballast minerals. *Deep-Sea Res. I* **49**: 219–236. doi:10.1016/S0967-0645(01)00101-1
- Bressac, M., C. Guieu, D. Doxaran, F. Bourrin, K. Desboeufs, N. Leblond, and C. Ridame. 2014. Quantification of the lithogenic carbon pump following a simulated dust-deposition event in large mesocosms. *Biogeosciences* **11**: 1007–1020. doi:10.5194/bg-11-1007-2014
- Burd, A. B., and G. A. Jackson. 2009. Particle aggregation. *Ann. Rev. Mar. Sci.* **1**: 65–90. doi:10.1146/annurev.marine.010908.163904
- Dickson, R. R., and I. N. McCave. 1986. Nepheloid layers on the continental slope west of Porcupine Bank. *Deep-Sea Res.* **33**: 791–818. doi:10.1016/0198-0149(86)90089-0
- Engel, A. 2000. The role of transparent exopolymer particles (TEP) in the increase in apparent particle stickiness (a) during the decline of a diatom bloom. *J. Plankton Res.* **22**: 485–497. doi:10.1093/plankt/22.3.485
- Engel, A., L. Abramson, J. Szlosek, Z. Liu, G. Steward, D. Hirschberg, and C. Lee. 2009a. Investigating the effect of ballasting by CaCO<sub>3</sub> in *Emiliania huxleyi*, II: Decomposition of particulate organic matter. *Deep-Sea Res. I* **56**: 1408–1419. doi:10.1016/j.dsr2.2008.11.028
- Engel, A., J. Szlosek, L. Abramson, Z. Liu, and C. Lee. 2009b. Investigating the effect of ballasting by CaCO<sub>3</sub> in *Emiliania huxleyi*: I. Formation, settling velocities and physical properties of aggregates. *Deep-Sea Res. I* **56**: 1396–1407. doi:10.1016/j.dsr2.2008.11.027
- Fischer, G., and G. Karakas. 2009. Sinking rates and ballast composition of particles in the Atlantic Ocean: Implications for the organic carbon fluxes to the deep ocean. *Biogeosciences* **6**: 85–102. doi:10.5194/bg-6-85-2009
- Fischer, G., C. Reuter, G. Karakas, N. Nowald, and G. Wefer. 2009. Offshore advection of particles within the Cape Blanc filament, Mauritania: Results from observational and modelling studies. *Prog. Oceanogr.* **83**: 322–330. doi:10.1016/j.pocean.2009.07.023
- Fischer, G., and others. 2016. Deep ocean mass fluxes in the coastal upwelling off Mauritania from 1988 to 2012:

- Variability on seasonal to decadal timescales. *Biogeosciences* **13**: 3071–3090. doi:10.5194/bg-13-3071-2016
- Fontaine, B., P. Roucou, M. Gaetani, and R. Marteau. 2011. Recent changes in precipitation, ITCZ convection and northern tropical circulation over North Africa (1979–2007). *Int. J. Climatol.* **31**: 633–648. doi:10.1002/joc.2108
- Francois, R., S. Honjo, R. Krishfield, and S. Manganini. 2002. Factors controlling the flux of organic carbon to the bathypelagic zone of the ocean. *Global Biogeochem. Cycles* **16**: 1087. doi:10.1029/2001GB001722
- Friese, C. A., M. van der Does, U. Merkel, M. H. Iversen, G. Fischer, and J. B. W. Stuut. 2016. Environmental factors controlling the seasonal variability in particle size distribution of modern Saharan dust deposited off Cape Blanc. *Aeolian Res.* **22**: 165–179. doi:10.1016/j.aeolia.2016.04.005
- Friese, C. A., J. A. van Hateren, C. Vogt, G. Fischer, J.-B. W. Stuut, H. van Hateren, C. Vogt, and G. Fischer. 2017. Seasonal provenance changes of present-day Saharan dust collected on- and offshore Mauritania. *Atmos. Chem. Phys.* **17**: 10163–10193. doi:10.5194/acp-2017-131
- Frignani, M., T. Courp, J. K. Cochran, D. Hirschberg, and L. Vitoria I Codina. 2002. Scavenging rates and particle characteristics in and near the Lacaze-Duthiers submarine canyon, northwest Mediterranean. *Cont. Shelf Res.* **22**: 2175–2190. doi:10.1016/S0278-4343(02)00078-X
- Goossens, D., and Z. Y. Offer. 2000. Wind tunnel and field calibration of six aeolian dust samplers. *Atmos. Environ.* **34**: 1043–1057. doi:10.1016/S1352-2310(99)00376-3
- Hall, I. R., S. Schmidt, I. N. Mccave, and J. L. Reyss. 2000. Margin: Implications for particulate organic carbon export. *Deep-Sea Res. I* **47**: 557–582. doi:10.1016/S0967-0637(99)00065-5
- Hamm, C. E. 2002. Interactive aggregation and sedimentation of diatoms and clay-sized lithogenic material. *Limnol. Oceanogr.* **47**: 1790–1795. doi:10.4319/lo.2002.47.6.1790
- Iversen, M. H., N. Nowald, H. Ploug, G. A. Jackson, and G. Fischer. 2010. High resolution profiles of vertical particulate organic matter export off Cape Blanc, Mauritania: Degradation processes and ballasting effects. *Deep-Sea Res. I* **57**: 771–784. doi:10.1016/j.dsr.2010.03.007
- Iversen, M. H., and H. Ploug. 2010. Ballast minerals and the sinking carbon flux in the ocean: Carbon-specific respiration rates and sinking velocity of marine snow aggregates. *Biogeosciences* **7**: 2613–2624. doi:10.5194/bg-7-2613-2010
- Iversen, M. H., and H. Ploug. 2013. Temperature effects on carbon-specific respiration rate and sinking velocity of diatom aggregates - potential implications for deep ocean export processes. *Biogeosciences* **10**: 4073–4085. doi:10.5194/bg-10-4073-2013
- Iversen, M. H., and M. L. Robert. 2015. Ballasting effects of smectite on aggregate formation and export from a natural plankton community. *Mar. Chem.* **175**: 18–27. doi:10.1016/j.marchem.2015.04.009
- Jickells, T. D., and others. 2005. Global iron connections between desert dust, ocean biogeochemistry, and climate. *Science* **308**: 67–71. doi:10.1126/science.1105959
- Karakaş, G., N. Nowald, M. Blaas, P. Marchesiello, S. Frickenhaus, and R. Schlitzer. 2006. High-resolution modeling of sediment erosion and particle transport across the northwest African shelf. *J. Geophys. Res.* **111**: C06025. doi:10.1029/2005JC003296
- Kiorboe, T. 2008. Particle encounter by advection, p. 57–82. *In* A mechanistic approach to plankton ecology. Princeton Univ. Press.
- Klaas, C., and D. E. Archer. 2002. Association of sinking organic matter with various types of mineral ballast in the deep sea; implications for the rain ratio. *Global Biogeochem. Cycles* **16**: 1116. doi:10.1029/2001GB001765
- Lampitt, R. S., and others. 2008. Ocean fertilization: A potential means of geoengineering? *Philos. Trans. R. Soc. A* **366**: 3919–3945. doi:10.1098/rsta.2008.0139
- Lee, C., and others. 2009. Particulate organic matter and ballast fluxes measured using time-series and settling velocity sediment traps in the northwestern Mediterranean Sea. *Deep-Sea Res. I* **56**: 1420–1436. doi:10.1016/j.dsr.2008.11.029
- Li, X., and B. E. Logan. 1997. Collision frequencies between fractal aggregates and small particles in a turbulently sheared fluid. *Environ. Sci. Technol.* **31**: 1237–1242. doi:10.1021/es960772o
- Li, X. Y., and B. E. Logan. 2000. Settling and coagulation behaviour of fractal aggregates. *Water Sci. Technol.* **42**: 253–258.
- Lucio, P. S., L. C. B. Molion, C. de Avila Valadao, F. C. Conde, A. M. Ramos, and M. L. Dias de Melo. 2012. Dynamical outlines of the rainfall variability and the ITCZ role over the west Sahel. *Atmos. Clim. Sci.* **2**: 337–350. doi:10.4236/acs.2012.23030
- Maher, B. A., J. M. Prospero, D. Mackie, D. Gaiero, P. P. Hesse, and Y. Balkanski. 2010. Global connections between aeolian dust, climate and ocean biogeochemistry at the present day and at the last glacial maximum. *Earth Sci. Rev.* **99**: 61–97. doi:10.1016/j.earscirev.2009.12.001
- McTainsh, G., and C. Strong. 2007. The role of aeolian dust in ecosystems. *Geomorphology* **89**: 39–54. doi:10.1016/j.geomorph.2006.07.028
- Mendez, M. J., R. Funk, and D. E. Buschiazzo. 2011. Field wind erosion measurements with Big Spring Number Eight (BSNE) and Modified Wilson and Cook (MWAC) samplers. *Geomorphology* **129**: 43–48. doi:10.1016/j.geomorph.2011.01.011
- Naiman, R. J. 1976. Primary production, standing stock, and export of organic matter in a Mohave Desert thermal stream. *Limnol. Oceanogr.* **21**: 60–73. doi:10.4319/lo.1976.21.1.0060
- Nowald, N., M. H. Iversen, G. Fischer, V. Ratmeyer, and G. Wefer. 2015. Time series of in-situ particle properties and sediment trap fluxes in the coastal upwelling filament off

- Cape Blanc, Mauritania. *Prog. Oceanogr.* **137**: 1–11. doi:[10.1016/j.pocean.2014.12.015](https://doi.org/10.1016/j.pocean.2014.12.015)
- Pabortsava, K., and others. 2017. Carbon sequestration in the deep Atlantic enhanced by Saharan dust. *Nat. Geosci.* **10**: 189–194. doi:[10.1038/ngeo2899](https://doi.org/10.1038/ngeo2899)
- Passow, U. 2004. Switching perspectives; do mineral fluxes determine particulate organic carbon fluxes or vice versa? *Geochem. Geophys. Geosyst.* **5**: Q04002. doi:[10.1029/2003GC000670](https://doi.org/10.1029/2003GC000670)
- Passow, U., and C. L. De La Rocha. 2006. Accumulation of mineral ballast on organic aggregates. *Global Biogeochem. Cycles* **20**: GB1013. doi:[10.1029/2005GB002579](https://doi.org/10.1029/2005GB002579)
- Ploug, H., and B. B. Jørgensen. 1999. A net-jet flow system for mass transfer and microsensor studies of sinking aggregates. *Mar. Ecol. Prog. Ser.* **176**: 279–290. doi:[10.3354/meps176279](https://doi.org/10.3354/meps176279)
- Ploug, H., S. Hietanen, and J. Kuparinen. 2002. Diffusion and advection within and around sinking, porous diatom aggregates. *Limnol. Oceanogr.* **47**: 1129–1136. doi:[10.4319/lo.2002.47.4.1129](https://doi.org/10.4319/lo.2002.47.4.1129)
- Ploug, H., M. H. Iversen, and G. Fischer. 2008a. Ballast, sinking velocity, and apparent diffusivity within marine snow and zooplankton fecal pellets: Implications for substrate turnover by attached bacteria. *Limnol. Oceanogr.* **53**: 1878–1886. doi:[10.4319/lo.2008.53.5.1878](https://doi.org/10.4319/lo.2008.53.5.1878)
- Ploug, H., M. H. Iversen, M. Koski, and E. T. Buitenhuis. 2008b. Production, oxygen respiration rates, and sinking velocity of copepod fecal pellets: Direct measurements of ballasting by opal and calcite. *Limnol. Oceanogr.* **53**: 469–476. doi:[10.4319/lo.2008.53.2.0469](https://doi.org/10.4319/lo.2008.53.2.0469)
- R Core Team. 2016. R: A language and environment for statistical computing. R Foundation for Statistical Computing. doi:[10.1007/978-3-540-74686-7](https://doi.org/10.1007/978-3-540-74686-7)
- Ridame, C., J. Dekaezemacker, C. Guieu, S. Bonnet, S. L'Helguen, and F. Malien. 2014. Contrasted Saharan dust events in LNLC environments: Impact on nutrient dynamics and primary production. *Biogeosciences* **11**: 4783–4800. doi:[10.5194/bg-11-4783-2014](https://doi.org/10.5194/bg-11-4783-2014)
- Riley, J. S., R. Sanders, C. Marsay, F. A. C. Le Moigne, E. P. Achterberg, and A. J. Poulton. 2012. The relative contribution of fast and slow sinking particles to ocean carbon export. *Global Biogeochem. Cycles* **26**: GB1026. doi:[10.1029/2011GB004085](https://doi.org/10.1029/2011GB004085)
- Shao, Y., and others. 2011. Dust cycle: An emerging core theme in Earth system science. *Aeolian Res.* **2**: 181–204. doi:[10.1016/j.aeolia.2011.02.001](https://doi.org/10.1016/j.aeolia.2011.02.001)
- Simon, M., H. P. Grossart, B. Schweitzer, and H. Ploug. 2002. Microbial ecology of organic aggregates in aquatic ecosystems. *Aquat. Microb. Ecol.* **28**: 175–211. doi:[10.3354/ame028175](https://doi.org/10.3354/ame028175)
- Stolzenbach, K. D. 1993. Scavenging of small particles by fast-sinking porous aggregates. *Deep-Sea Res. I* **40**: 359–369. doi:[10.1016/0967-0637\(93\)90008-Q](https://doi.org/10.1016/0967-0637(93)90008-Q)
- Ternon, E., C. Guieu, M.-D. Loÿe-Pilot, N. Leblond, E. Bosc, B. Gasser, J.-C. Miquel, and J. Martín. 2010. The impact of Saharan dust on the particulate export in the water column of the North Western Mediterranean Sea. *Biogeosciences* **7**: 809–826. doi:[10.5194/bg-7-809-2010](https://doi.org/10.5194/bg-7-809-2010)
- Wilson, S. J., and R. U. Cooke. 1980. Wind erosion, p. 217–251. *In* M. J. Kirkby and R. P. C. Morgan [eds.], *Soil erosion*. Wiley.

#### Acknowledgments

We thank Christiane Lorenzen for the POC measurements and the crew of the R/V *Poseidon* POS481 for assistance during the cruise. This study was supported by the Helmholtz Association (to HJ and MHI), the Alfred Wegener Institute Helmholtz Centre for Polar and Marine Research (to HJ and MHI) and the DFG-Research Center/Cluster of Excellence “The Ocean in the Earth System” at MARUM (to all). This publication is supported by the HGF Young Investigator Group SeaPump “Seasonal and regional food web interactions with the biological pump”: VH-NG-1000.

#### Conflict of Interest

None declared.

Submitted 05 May 2017

Revised 19 October 2017

Accepted 11 December 2017

Associate editor: Thomas Kiørboe